

Integrated Microfluidic and Optical Sorting Device

Vuong Hoang Kim¹, Nguyen Manh Huy¹ and Gani Zhi Hao Terry¹

¹National University of Singapore High School of Mathematics and Science

20 February 2009

Abstract

Introduced in 1969, optical force method utilizes a focused **Electromagnetic Beam** to exert forces on microparticles, allowing them to be easily manipulated. This **non-invasive** and **sterile** [1] method requires no other mechanical support, making it an ideal choice for handling sensitive samples in many biophysics applications. Furthermore, since the strength of the force varies with particles properties such as **flow speed, size, refractive index** [1], this method proves itself extremely useful in sorting **microparticles**. With yeast cells as the primary subject, we attempt to use the above technique to isolate and purify a wide range of microparticles. The system comprises a network of crossed, coupled channels casted in poly(dimethylsiloxane) (PDMS) and an infrared laser beam emerging from the objective lens in an optical microscope. When suspended microparticles matching specific criteria approach the junction from the lower channel, they are **pushed to the upper channel by the optical force** due to the laser beam. We aim to formulate the optimal parameters, namely flow rate, size and laser power, required for maximum sorting efficiency, which could be used as a reference for further industrial developments.

1 Background

Microparticles in general refer to all particles, whether inorganic, polymeric or biological, for example yeast cells and microsized silica beads. It is of great interest in several fields to separate microparticles of different sizes. For instance, many biomedical applications involve separation of cells of interest from a larger mixed population for further processing. There have been many methods proposed so far for the purpose of separating microparticles of different sizes, one of which is the use of optical force. First used in 1969, it involves using a focused electromagnetic beam to exert forces on microparticles. The force exerted depends on the particles properties such as particle size, refractive index and flow speed, and hence different particles experience different forces and can be separated efficiently. Examples of the use of this concept are optical potential energy landscapes [2–5], optical chromatography [6, 7], single spot optical tweezers [1, 8, 9] and microfluidic sorting, the focus of this paper. As it uses optical force, this method is non-invasive, sterile and does not require other mechanical support, an advantage over electrokinetically actuated techniques [10]. Furthermore, no labelling of particles is required, minimum degradation of particles occurs and, making it an ideal choice for many biophysics applications. It also has advantages over other techniques involving optical force, as it can manipulate and sort multiple particles at the same time in a relatively fast flow environment, and particles can be readily collected at different reservoirs of outlets.

The entire sorting process can be done on a **small chip comprising a network of crossed and coupled channels** cast in poly(dimethylsiloxane) (PDMS). This system eliminates the need for large fractionating arrays or long channels. PDMS is ideal for this application as it is optically clear, inert, non-toxic and non-flammable [11]. The optical force is produced by an infrared laser beam emerging from the objective lens in an optical microscope. When suspended microparticles matching specific criteria approach the junction from the lower channel, **they are pushed to the upper channel by the optical force due to the laser beam**. Success has been achieved in sorting synthetic silica microparticles. However, this method has not been applied in optimal sorting of yeast cells in the industry yet. Success of this endeavour is essential for the advancement of further industrial processes, microfluidic-based life science research and diagnostic platforms.

2 Purpose

Our project aims to investigate the optical parameters, namely flow rate and size to maximise sorting efficiency. After a general literature review of existing methods and techniques, the investigation of the optical parameters for sorting efficiency would be carried out. For our experiments, yeast cells were used as subjects.

3 Methods

The procedure consists of three main steps: firstly, **the fabrication of the PDMS chips** in which the experiment is carried out. Secondly, the actual experimental procedure in which **microparticles are introduced into the PDMS chips** and finally, the **calculation of their sizes and exact speeds** for further analysis.

In order to produce the PDMS chips, a master mould made of silicon wafer was fabricated using the proton beam writing technique as shown in Figure 1 [12]. With this master, a large number of identical PDMS chips can be produced readily and rapidly. The master was placed in a small plastic tray and liquid PDMS, mixed with curing agent in a 10:1 ratio and heated until hardening. The master was then slowly and carefully detached from the hardened PDMS, leaving the sample with the inverse structures of the master mould. Holes were then inserted using a Harris Uni-Core punch at appropriate locations along the channels, providing inlets and outlets for the microfluidic flow. Two such pieces of PDMS were sonicated in ethanol and exposed to plasma for 20s (Harrick Plasma Cleaner in Figure 11). Next, the two PDMS channels were then bonded to each other to provide a junction for separation of microparticles. Lastly, the sample was bonded to a glass slide as a base and heated in an oven at 80 °C for at least one hour.

For the experimental procedure, yeast cells of different sizes, suspended in an aqueous solution, were introduced into the lower channel, while deionized water was introduced in the upper channel. The flow was controlled by a syringe pump. It was observed that the fluid flowed straight through the intersection without significant exchange of fluid between the channels when the aspect ratio of the microchannels was high (e.g. 1.6) [13].

To better understand the operation of this device, one should consider the forces acting on these cells as they enter the “sorting box.” When cells encounter the line laser, they are rapidly slowed down by a **gradient force**. If this gradient force is sufficiently strong, the cells can be stopped or slowed to a very low speed and pushed up by a scattering force which acts perpendicular to the fluidic flow. This scattering force increases as the **size, refractive index of the cells and intensity of the laser beam** increase. For an objective lens with a low numerical aperture, the scattering force is much stronger than gradient force [8], resulting in cells being deflected to upper channel rather than trapped at the focus. These two forces are the main mechanism for this microfluidic device.

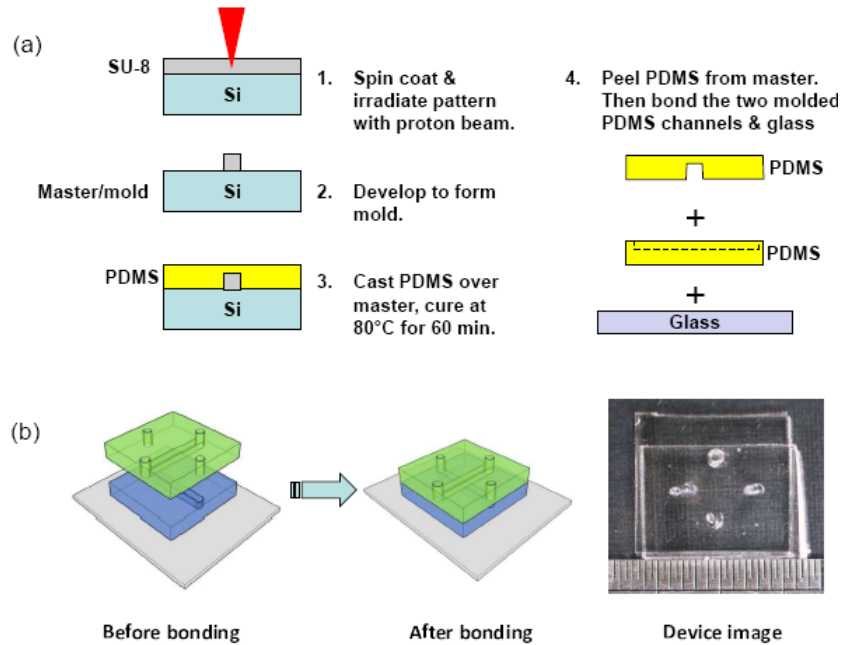


Figure 1: Process of making the chips

When the cells move up, they will be pushed along by the sustained flow in the upper channel. The simple operation of the device illustrated in Figure 2 enables automated sorting of yeast cells efficiently without the need to turn off or translate the laser beam. As a focused single spot laser is only effective in its immediate surroundings, a cylindrical lens was incorporated into the optical train to spread the beam into a line [14] spanning the entire width of the sorting box, significantly increasing the sorting efficiency by allowing multiple particles to be sorted simultaneously.

Lastly, for the data analysis, yeast cells were flowed through the sorter according to the procedure above. Apart from the intrinsic variation in size of the yeast cells, the flow rate was varied between experiments using the syringe pump. Even in the same sample, yeast cells were observed to flow at different rates. This gives a good variation of parameters in the samples experimented upon. The captured videos of flow were decompiled into jpeg files using *VirtualDub*. An IDL program was used to determine the flow rate of the yeast cells from the jpeg files obtained, correcting for aspect ratio and zoom factor. The parameters for the cells were then tabulated and the correlation between each of the parameters and sorting efficiency was statistically determined, as presented subsequently.

4 Results and Analysis

The performance of this sorting system under a 60X lens is illustrated in Figure 3, based on statistical analysis of 1000 yeast cells. Larger cells (diameter greater than 3 μm) are sorted efficiently (70% to 90%) at speeds below 150 $\mu\text{m}/\text{s}$. At speeds higher than this switching speed the efficiency percentage decreases gradually. Very few large cells are switched when the speed is greater than 275 $\mu\text{m}/\text{s}$. The same observation also applies for smaller cells (diameter less than 3 μm). However, their switching percentage is always lower as the optical force on them is weaker. Sorting efficiency for smaller cells drops more rapidly than larger cells and reaches essentially

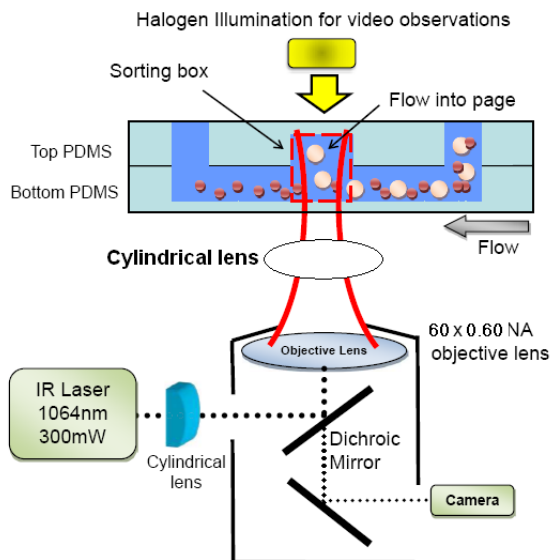


Figure 2: Schematic of optical sorting microfluidic system with focused laser applied at the junction of the two overlapping channels

zero at speeds above $250 \mu\text{m/s}$.

An outcome-based figure of merit (FOM) is constructed to indicate how well large and small cells are separated as a function of flow speed. We denote A as the percentage of large yeast cells that were switched successfully by the laser beam over all the large cells in the mixed solution and B as the percentage of small yeast cells that were switched over all small cells in the mixture. The FOM is defined as $(A - B)$. At low speed ($25 \mu\text{m/s}$ - $100 \mu\text{m/s}$) this difference is small ($< 20\%$) as both large and small yeast cells are pushed to the upper channel by the laser force. However, as the flow speed increases, the gradient force is no longer strong enough to slow down the faster-moving small cells in order for the scattering force to switch them to the upper channel. This effect at higher speed is less pronounced for larger cells due to their bigger sizes. As a result, the FOM gradually increases and reaches a maximum (51%) within the speed range of $175 \mu\text{m/s}$ to $200 \mu\text{m/s}$. At speeds higher than this, both large and small cells move too fast for the gradient force to slow them down sufficiently and for the scattering force to switch them. Hence, the FOM decreases and tends to zero at very high speed.

The size distribution of yeast cells, characterized by their diameters, in the sorting process is also analyzed and presented in figures 4 to 6. Before sorting, the unimodal size distribution peaks at 3 to $4 \mu\text{m}$, which is the typical diameter of a yeast cell. Upon sorted, there is an excess of smaller cells in the lower channel, which shifts the peak in the size distribution towards lower values. In contrast, most large cells and very few small cells are switched to the upper channel, characterized by a lower percentage of cells in the range of 1 to $3 \mu\text{m}$, compared to the normal distribution.

In the sequence of images in Figure 7, the paths of a single large cell (circled in blue) and a single small cell (circled in red) are tracked as they transverse the flow. After the junction the large cell is switched to the upper channel while the small one continues in its path.

In the three images illustrated in Figure 8, trajectories of yeast cells are plotted as they approach and exit the sorting box, which is $50 \times 50 \times 60 \text{ mm}^3$ in dimensions. The white arrows show the direction of fluid flow while the solid lines represent small cells and crosses represent large cells. In image (a) with the absence of laser, large cells keep flowing in the bottom channel

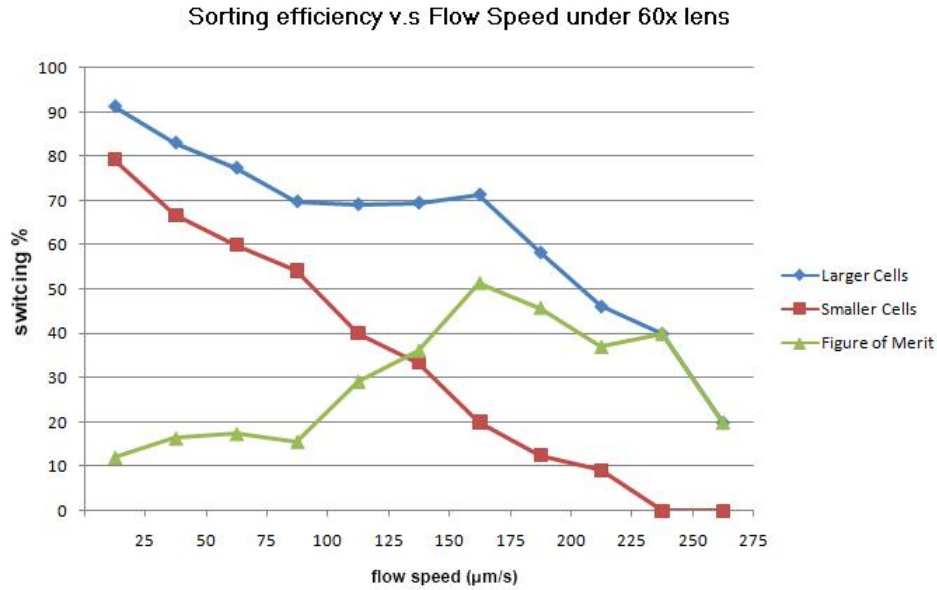


Figure 3: Graph of sorting efficiency versus flow speed under 60X lens

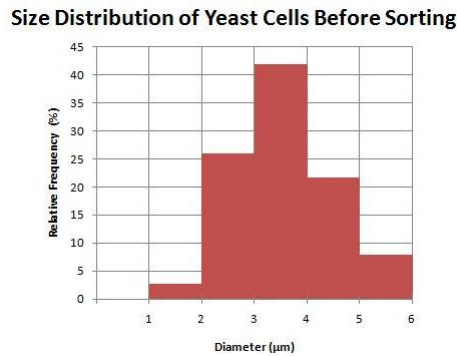


Figure 4: Graph of relative frequency versus flow (Before sorting)

while some of the smaller cells may escape from the flow and switch to the upper channel. In the presence of a 300-mW 1064-nm line laser, indicated by the red dotted line, images (b) and (c) present the trajectories of small and large yeast cells respectively.

We repeated this experiment with a 40X lens. Generally high switching percentage occurs at lower speeds compared to using a 60X lens. Larger cells (diameter greater than 3 μm) are sorted efficiently (70 to 90%) at speeds below 100 $\mu\text{m/s}$. More than half of small cells are switched if their speeds are lower than 50 $\mu\text{m/s}$. The maximum sorting efficiency, indicated by a peak in the FOM, is achieved in the range of 75 to 100 $\mu\text{m/s}$. Due to the weaker laser intensity produced by the 40X lens, switching percentage for both large and small cells drops much faster than compared to the 60X lens, reaching essentially zero at speed greater than 175 $\mu\text{m/s}$.

Size Distribution of Yeast Cells After Sorting In the Upper Channel

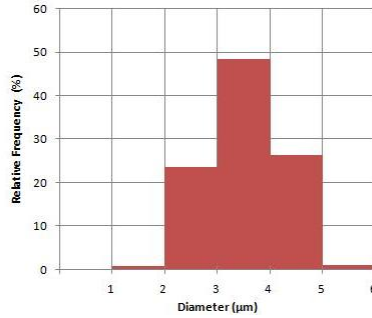


Figure 5: Graph of relative frequency versus flow (After sorting in the upper channel)

Size Distribution of Yeast Cells After Sorting In the Lower Channel

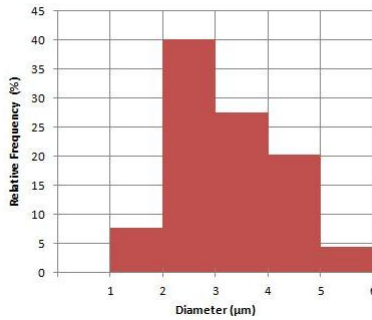


Figure 6: Graph of relative frequency versus flow (After sorting in the lower channel)

5 Discussion

We have encountered many difficulties while carrying out this project. At first it took us great effort to create ideal flows in both channels. Subsequently by using an automated syringe pump we had greater control over the flow speed and obtain relatively laminar fluidic flows. The bond between PDMS surfaces was initially weak and required us to handle them with great care. Weak bonding also could not stand relatively high water pressure in the channels. After many trials, however, we found out the optimal plasma exposure time and vacuum pressure during fabrication to give the PDMS very strong bonding. Several times during manual detachment of casted PDMS channels from the master, incorrect pressure may result in the breakage of the fragile silicon master mold or decortications of the SU-8 lines on the master surface. The thickness of the PDMS chips also requires much attention. Too thin chips have limited mechanical endurance while too thick chips degrade imaging quality and hampers experiments using short working distance lens. The very solution flowing in the channel can also absorb laser energy and heat up the channels to the point of destruction. After trying various solutions, including ethanol, isopropanol and acetone, we decided that deionized water is the best solvent to use. Data analysis with IDL also presents a major problem as all the images are displayed in grayscale with low resolution, making trajectory tracking and speed calculation difficult.

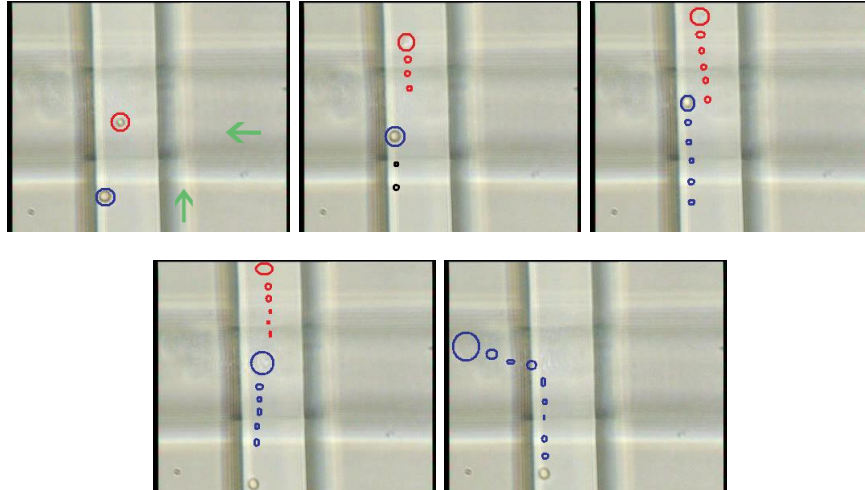


Figure 7: Trajectory paths of single large and small cells within channel

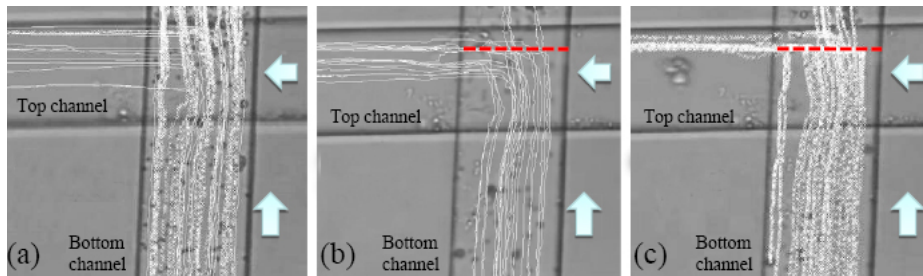


Figure 8: Trajectory path of yeast cells in the absence and presence of laser

6 Conclusion

We have successfully developed a versatile and effective method for sorting yeast cells using a microfluidic system. The separation is efficient and shows the great potential of this device to separate yeast cells according to size, which only requires adjusting the flow speed and laser power.

7 Future Extensions

A possible extension the group is investigating is the use of this system to fractionally remove impurities (spherical particles) from pure Zinc oxide nanowires (rod-like particles) due to the difference in their geometrical shapes. This method can also be applied to sorting biological cells as their sizes generally range from 8 to 10 μm . The laser beam can be further modified by multiplexing a high-powered laser beam to multiple “sorting junctions” on a chip, enabling the possibility of parallel sorting with a higher throughput.

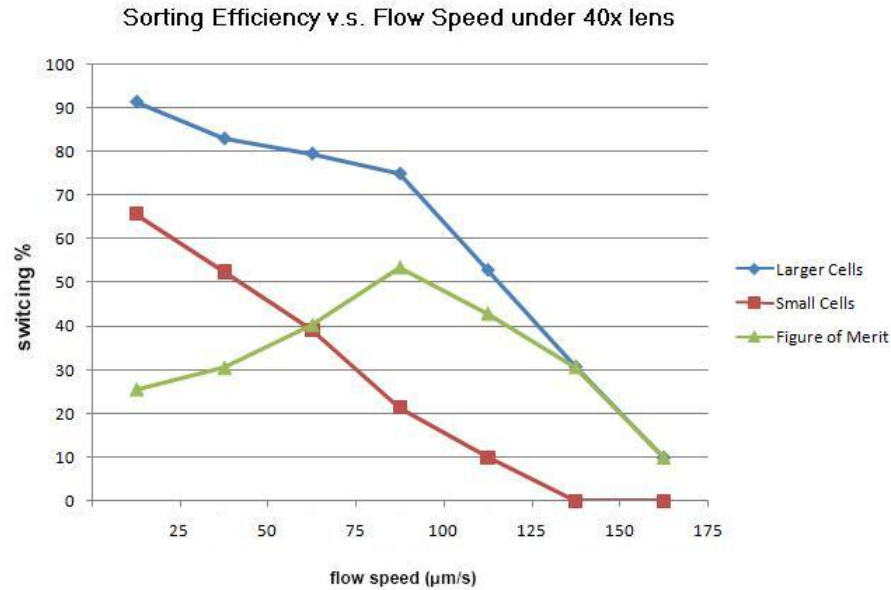


Figure 9: Graph of sorting efficiency versus flow speed under 40x lens

References

- [1] S. K. Hoi, C. Udalgama, C.-H. Sow, A. A. Bettiol, and FrankWatt, *Applied Physics B (Laser and Optics)* **90**, 131 (2008).
- [2] M. P. MacDonald, G. C. Spalding, and K. Dholakia, *Nature* **426**, 421 (2003).
- [3] K. Ladavac, K. Kasza, and D. G. Grier, *Phys. Rev. E* **70**, 010901 (2004).
- [4] A. M. Lacasta, J. M. Sancho, A. H. Romero, and K. Lindenberg, *Phys. Rev. Lett.* **94**, 160601 (2005).
- [5] R. L. Smith, G. C. Spalding, K. Dholakia, and M. Macdonald, *J. Opt. A: Pure Appl. Opt.* **9**, 134 (2007).
- [6] S. J. Hart, A. V. Terray, J. Arnold, and T. Leski, *Opt. Express* **15**, 2724 (2007).
- [7] S. J. Hart, A. V. Terray, and J. Arnold, *Appl. Phys. Lett.* **91**, 171121 (2007).
- [8] J. Oakey, J. Allely, and D. W. M. Marr, *Biotechno. Prog.* **18**, 1439 (2002).
- [9] J. Enger, M. Goksor, K. Ramser, P. Hagberg, and D. Hanstorp, *Lab on a Chip* **4**, 196 (2004).
- [10] C. Lin, A. Chen, and C. H. Lin, *Biomed Microdevices* **10**, 55 (2008).
- [11] L. Wang, L. A. Flanagan, N. L. Jeon, E. Monuki, and A. P. Lee, *Lab on a Chip* **7**, 1114 (2007).
- [12] Wikipedia, "Polydimethylsiloxane — wikipedia, the free encyclopedia," [Online; accessed 8-December-2008].

- [13] J. A. van Kan, L. Wang, P. Shao, A. A. Bettiol, and F. Watt, Nucl. Instr. and Meth. In Phys. Res. B **260**, 353 (2007).
- [14] R. F. Ismagilov, D. Rosmarin, P. J. A. Kenis, D. T. Chiu, W. Zhang, H. A. Stone, and G. M. Whitesides, Anal. Chem. **73**, 4682 (2001).

8 Appendix

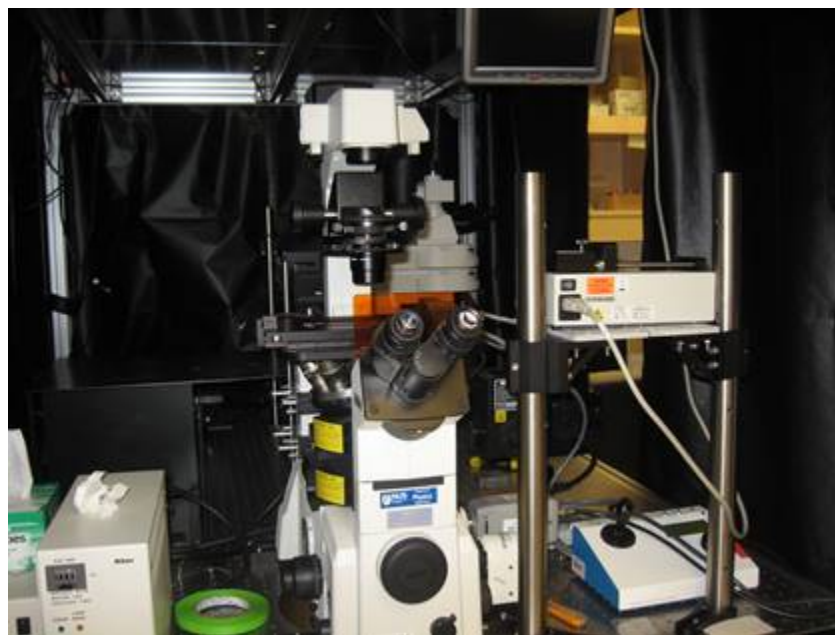


Figure 10: Nikon TE2000-U Microscope



Figure 11: Harrick Plasma Cleaner



Figure 12: Syringe pump

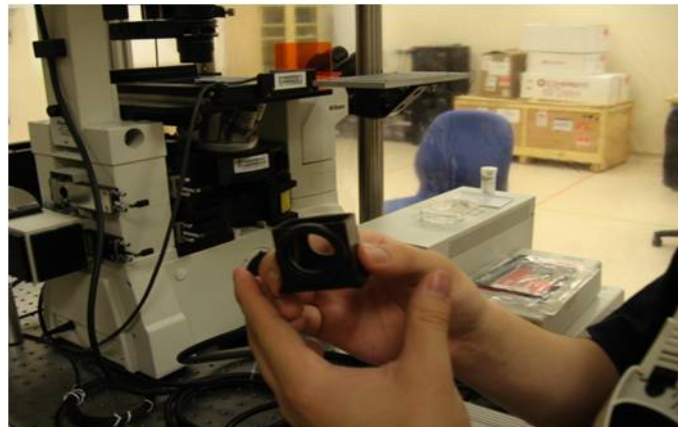


Figure 13: Dichroic mirror



Figure 14: Sonicator

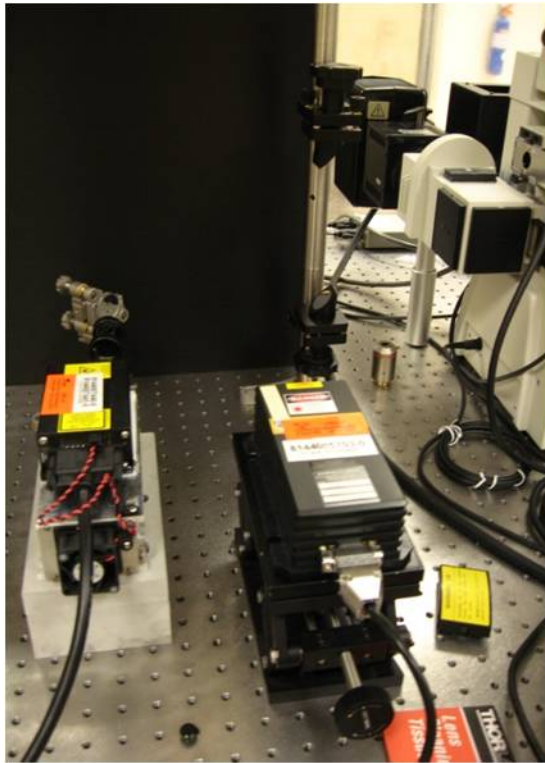


Figure 15: Laser generator